



Development of lateral flow membranes for immunoassay separation

A.L. Ahmad^{a*}, S.C. Low^a, S.R. Abd Shukor^a, A. Ismail^b, A.R. Sunarti^a

^aSchool of Chemical Engineering, Engineering Campus, Universiti Sains Malaysia, Seri Ampangan, 14300 Nibong Tebal, S.P.S, Penang, Malaysia

Tel: +6 04 594 1012, Fax: +6 04 594 1013; email: chlatif@eng.usm.my

^bInstitute for Research in Molecular Medicine, Health Campus, Universiti Sains Malaysia, 16150 Kubang Kerian, Kelantan, Malaysia

Received 9 September 2008; Accepted 10 March 2009

ABSTRACT

The lateral flow nitrocellulose membrane is one of the commonly used separation media for bacteria detection in drinking water treatment facilities. In order to enhance its performance, control of the membrane surface and cross-section morphology is primarily important. The challenge of this study is to combine various formulations and casting variables to obtain lateral flow nitrocellulose membranes with the desired morphologies. Through the dry-phase inversion method, the drying temperature was found to be an important parameter in synthesizing membranes as it affects pore structures. A high drying temperature causes agglomeration of the polymer matrix, and thus smaller pores were observed on the membrane surface. This further decreases the membrane lateral liquid migration rate, besides reducing the membrane binding ability for bacteria detection. Results show that by decreasing polymer concentration, membrane surface pores became apparently larger, thus creating a faster lateral migration speed of the water solution. A larger pore size increases the chance for the bacteria detecting agent to bind onto the pore layers, which ultimately enhances the bacteria detection ability of the device.

Keywords: Membrane; Morphology; Microfiltration; Binding ability; Lateral flow

1. Introduction

Virus and bacteria detection in drinking water has brought water quality analysis to a whole new perspective due to waterborne outbreaks [1] such as typhoid fever [2], *Escherichia coli* O157 [3], *Giardia* and *Cryptosporidium* [4]. These typical waterborne viruses, even in very low concentration, may be lethal [4]. Hence, there is an urgent need to detect the presence of viruses and bacteria in water by a sensitive, reliable and efficient method.

Membrane separation technologies such as ultrafiltration (UF), microfiltration (MF) and reverse osmosis

(RO) are known as effective ways to detect low concentrations of viruses in wastewater treatment processes for the past decades [4]. A simple and rapid test strip was developed to detect the presence of selected viruses or bacteria in drinking water [5,6]. However, the developed immunological test strips are not able to cater to applications since different membrane materials, surface properties, structure and dimensions are required for different applications and different analyses.

In membrane technology, the most commonly used and important class of membrane fabrication method is the phase inversion technique [7,8]. Phase inversion refers to the process in which a polymer solution (liquid phase) inverts into a swollen, three-dimensional macromolecular

*Corresponding author.

network (solid state) [8,9]. The membrane formation mechanism was said to be rather complex as there are various fabrication factors to be considered during the casting stage, and its final performance strongly depends on the membrane fabrication method and the casting conditions. Manipulation of phase inversion [10] and fabrication factors including choices of casting materials [11], polymer concentration, membrane thickness [12], evaporation time and evaporation temperature are among parameters that directly influence the membrane's final performance.

Polymer concentration is the key factor that tailors membrane structures (morphology and pore size) and final membrane performances (membrane binding ability and liquid lateral migration speed) [13,14]. Viscosity of the casting dope increases when polymer concentration is increased. This results in the reduction of macrovoid formation in the membrane layers. On the other hand, in dry phase inversion, membrane drying temperature determines the thickness of membrane skin layer which eventually forms varying membrane structures.

Current study elucidates the influences of polymer concentration and drying temperature on membrane microstructure. Experimental works were carried out to investigate the effects of these two important elements against membrane morphology and its performance as transport medium for immunological membrane application. This improved membrane formation understanding can be used for future development of a highly efficient immunodiagnostic test strip to detect viruses or bacteria in drinking water.

2. Materials and methods

2.1. Materials

The nitrocellulose (NC) polymer used in this study contained 11.8–12.3% nitrate with 30% alcohol (Sigma, St. Louis, Mo). The solvent, methyl acetate (MA) and nonsolvent, isopropanol (IP) were purchased from Merck (Darmstadt, Germany), while distilled water and glycerol (Merck) were used as the pore former and additive in the casting dope. Bovine serum albumin (BSA) was purchased from Sigma, and the biconchonic acid working reagent (BCA) was purchased from Merck. The 0.05 M buffer tris (hydroxymethyl) aminomethane / HCl and 0.05 M phosphate buffer at pH 7.0 were prepared for characterization. The chemical structure of nitrocellulose polymer is as shown in Fig. 1.

2.2. Membrane preparation

NC membranes were prepared using the dry-phase inversion method [7,8,10]. In order to investigate the

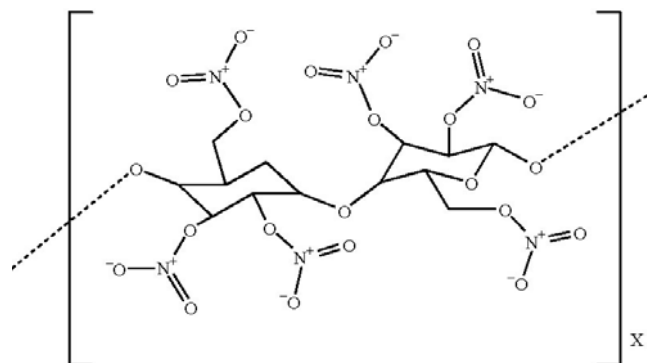


Fig. 1. Chemical structure of the nitrocellulose polymer.

effects of polymer concentration on membrane morphology, the weight fraction of the solvent was kept constant at 80 wt.% while the weight percentage of the polymer varied from 4 wt.% to 6 wt.%. The casting solutions were then allowed to dry within the heating chamber from 27°C to 53°C. Nine different compositions of casting dope used in this experiment are shown in Table 1. The casting process was carried out at ambient temperature using a membrane auto-casting machine set at 100 rpm casting speed.

2.3. Membrane characterization

Microstructures of fabricated flat-sheet membranes were confirmed by field emission scanning electron microscopy (VPFESEM, Supra 35VP, Germany). Membrane samples were first coated with a conducting layer, mainly to prevent the surface from being charged up. Average pore size was obtained and measured from the images.

The membrane porosity (ϵ) was calculated as follows [15,16]:

$$\epsilon = 1 - \frac{V_E}{V_A} \times 100\% \quad (1)$$

A flat-sheet membrane was cut into a 2×2 cm sample, and its thickness was measured. V_A , the apparent volume of the membrane, was calculated from the film thickness and the film surface area (2×2 cm). The existent volume of the membrane, V_E , was determined from the corresponding polymer density (1.23 g cm⁻³) and the polymer weight of the membrane sample. To ensure firm reproducibility of experimental data, five different locations were selected for the membrane porosity calculation.

2.4 Membrane performance test

In-plane liquid distribution or liquid lateral wicking time measurement was done on 2 cm wide and 10 cm long

Table 1
Membrane casting dope composition

Component	Casting dope composition								
	1	2	3	4	5	6	7	8	9
Polymer (wt.%)	4	4	4	5	5	5	6	6	6
Solvent (wt.%)	80	80	80	80	80	80	80	80	80
Nonsolvent + additives (wt.%)	16	16	16	15	15	15	14	14	14
Membrane drying temperature (°C)	27	40	53	27	40	53	27	40	53
Membrane evaporation time (min)	5	5	5	5	5	5	5	5	5
Initial cast thickness (μm)	700	700	700	700	700	700	700	700	700

membrane strips cut from the synthesised NC membrane. Medium used for wicking was deionized water or phenol red buffer solution consists of phenol red (Sigma) dissolved in 0.05 M tris(hydroxymethyl)aminomethane/HCl buffer solution. Phenol red buffer was used for better visibility of the migration front. The experiment was conducted at room temperature (27°C) and ambient pressure. Time was taken when the wicking medium had migrated 2-, 3-, and 4-cm standard wise after initial contact between the membrane and test medium.

In addition, the membrane protein binding ability was measured on 12-mm diameter samples and the total volume of membrane samples was calculated. Membrane samples were incubated in 3 ml of BSA with phosphate buffer (pH 7.0, mg/ml) and shaken for 3 h at 25°C. Unbound BSA on the membrane surfaces was then washed out (repeated two times) with phosphate buffer. Each sample replicate was transferred into a test tube with 2 ml BCA working reagent and then incubated at 37°C for 30 min. The liquid content was detected using a spectrophotometer at a wavelength of 562 nm. By using the standard curve from a previous preliminary study, the protein quantity of the membrane was calculated.

3. Results and discussion

3.1. Membrane characterization

Fig. 2 shows the effect of casting composition and casting condition by varying the polymer concentration from 4 wt.% to 6 wt.% at three different membrane drying temperatures, i.e. from 27°C to 54°C. Overall, by increasing the polymer concentration, synthesized membrane bulk porosity was increased. At a constant drying temperature (27°C), the membrane porosity was increased from 72.8% at 4 wt.% of nitrocellulose polymer to 76.5% at 6 wt.%. This increase in membrane bulk porosity is mainly caused by increasing membrane thickness, as shown in Table 2. For example, at 27°C drying temperature, the membrane synthesized from 4 wt.% of nitrocellulose polymer forms a membrane thickness of 89 μm . However,

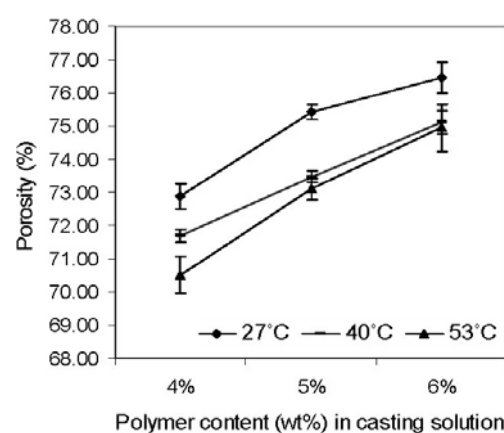


Fig. 2. Variation in the porosity of nitrocellulose membranes prepared with different casting compositions and conditions. Each porosity value represents an average value of five samples and the bars represent standard error.

with the additional 2 wt.% of membrane polymer (total 6 wt.%), the final membrane thickness was increased almost double to 163 μm . This significant increase in membrane thickness causes some macrovoid formation in the membrane layers, as discussed in previous work [12]. The size of the macrovoid is not as large as observed in the previous work [12]. However, a more porous membrane structure can still be observed from Fig. 3(F). This formation of macrovoids further increases the membrane bulk porosity.

Although the overall bulk porosity was increased with increasing polymer concentration in the casting solution, the membrane pore size gave an opposite observation. As expected, the membrane surface pore size decreased with an increased of polymer concentration. At 40°C drying temperature, membranes with low polymer concentration (4 wt.%) formed an average membrane surface pore size of 6.34 μm , as shown in Table 2. These membrane pores were considerably large compared to 5.54 μm and 4.90 μm when the NC polymer concentration was increased to 5 wt.% and 6 wt.%, respectively. During dry phase inversion, the polymer concentration on the air-side of the membrane surface was increased due to the loss of

Table 2
Membrane characterization

Polymer content ^a , wt%	Cast solution drying temperature, °C					
	27		40		53	
	Synthesized membrane thickness, μm	Membrane pore size, μm	Synthesized membrane thickness, μm	Membrane pore size, μm	Synthesized membrane thickness, μm	Membrane pore size, μm
4	89 ± 3	9.10 ± 0.29	117 ± 4	6.34 ± 0.37	101 ± 1	4.67 ± 0.26
5	103 ± 4	7.23 ± 0.49	113 ± 8	5.54 ± 0.05	118 ± 5	4.34 ± 0.25
6	163 ± 5	5.43 ± 0.01	156 ± 3	4.90 ± 0.08	167 ± 3	3.59 ± 0.08

^aInitial membrane cast thickness at 700 μm and average of five measurements for each membrane.

solvent. The higher polymer content in the casting solution causes thicker skin layer on the membrane surface, which further creates small membrane pores.

The effect of the membrane drying temperature was investigated by increasing the temperature of the heating chamber from 27°C to 53°C. At a constant casting composition, the drying temperature did not significantly affect the final membrane thickness, as shown in Table 2. In the porosity measurement, the membrane porosity decreases with the increase of drying temperature (Fig. 2). At a higher drying temperature, the rapid solvent diffusion rate hastens the polymer precipitation process and forms a highly concentrated polymer near to the membrane surface area [17,18]. This leads to the formation of smaller pores on the membrane surface and lower membrane bulk porosity.

3.2. Effects of casting conditions on membrane morphologies

To validate and understand the kinetic phenomena that occurred during the dry phase inversion process, field emission scanning electron microscopy (FESEM) was adopted to visualize the membrane morphology. Fig. 3 shows a series of membranes morphologies prepared at different polymer concentrations. All membranes present a porous and three-dimensional open pore structure. Surface micrographs revealed that a membrane with 4 wt% of nitrocellulose polymer appeared to have a large pore size. With increasing polymer concentration in the casting solution, the membrane surface pores became smaller and the membrane became thicker, as shown in Fig. 3. Theoretically, polymer distribution at the onset of precipitation provides a dense skin layer near the membrane–air interface [19]. With increasing polymer content, the membrane top layer needs to support larger polymer precipitation and interfacial stresses, hence creating smaller pores on the top surface.

Both Fig. 3(D–F) and Table 2 show that when polymer concentration is increased, the membrane thickness

increases as well. Two factors affecting the increase in membrane thickness are: (1) the addition of polymer weight percentage in the casting solution that increases the solid content in the membrane; and (2) when more polymer precipitates on the membrane top surface, it slows down the outward diffusion of the solvent and thus creates macrovoids in the membrane layers [17]. In contrast, at low polymer concentration, lower solids content and non-macrovoid formation in the membrane layers results in a thinner membrane thickness.

In the present work, it is observed that for the range of 27°C to 53°C, the overall membrane thickness was not significantly influenced by the membrane drying temperature (FESEM results are not displayed). As described before, the increase of drying temperature results in higher polymer precipitation on the membrane top surface and thus slows down the outward diffusion of the solvent. Theoretically, the membrane thickness is supposed to be increased. However, during high temperature drying, the polymer matrix of the membrane tends to agglomerate. Consequently, it further decreases the connection voids between the membrane layers and contributes to lower membrane thickness. This contradicting behaviour is the main reason why membrane thickness is independent from the drying temperature.

In Fig. 4(A–C), at a constant polymer content of 5 wt.%, the surface pores of the membrane formed by a low drying temperature (27°C) are larger than membranes formed at a higher drying temperature (53°C). This high drying temperature accelerates the separation process, which creates polymer agglomeration close to the top layer. It is the fast outward diffusion of the solvent that is responsible for the decreasing membrane pore size against high drying temperatures.

3.3. Membrane performance

The effects of casting composition and conditions on membrane lateral wicking performance are as illustrated

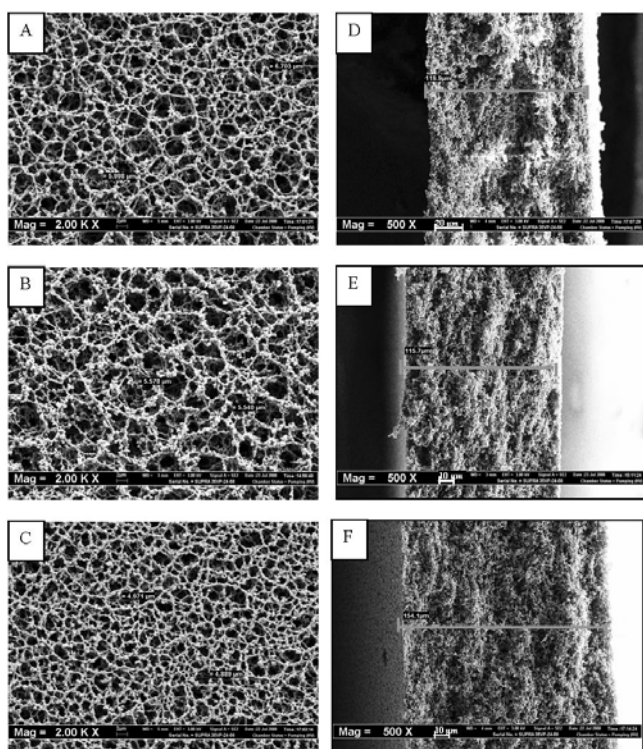


Fig. 3. FESEM micrograph of the (left) membrane surface structure and (right) cross sectional structure of nitrocellulose polymer contents for (A) 4.0, (B) 5.0, and (C) 6.0 wt% in casting solutions (at a constant 40° of drying temperature).

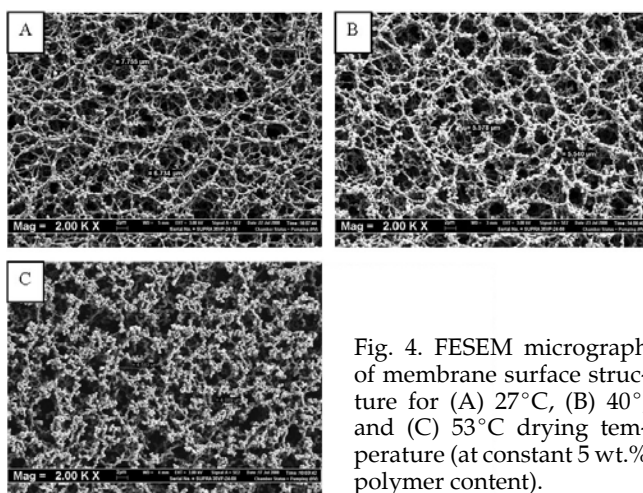


Fig. 4. FESEM micrograph of membrane surface structure for (A) 27°C, (B) 40°, and (C) 53°C drying temperature (at constant 5 wt.% polymer content).

in Fig. 5(a) and (b). In general, the membrane lateral wicking performance demonstrates the same behaviour for both testing media (water and phenol red solution). Based on the experimental results in Fig. 5(a), membrane lateral wicking time was increased from 490 s to 811 s at 40°C when the polymer concentration was increased from 4 wt.% to 6 wt.%. As shown previously in Table 2, the increases of polymer content in casting solution caused

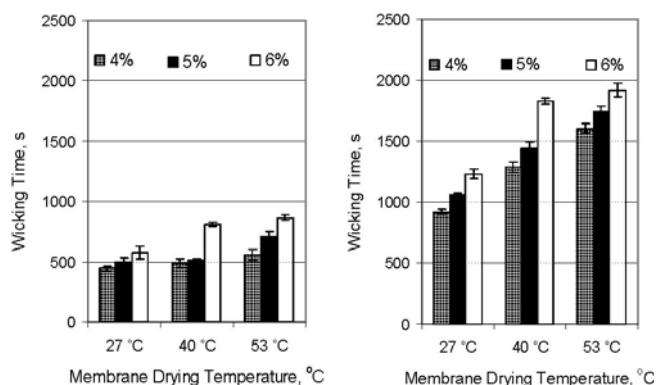


Fig. 5. Wicking time needed for the testing media: (a) water (b) phenol red to migrate to 4 cm height on the membrane strips prepared at different drying temperatures (27°C, 40°C, 50°C) and different polymer concentrations (4 wt.%, 5 wt.%, 6 wt.%). Bars represent the standard error.

the formation of membrane with smaller pore size. As a result, the membrane exhibits more resistance in lateral liquid flow across membrane layers and at the end converts to longer lateral wicking time.

Apparently, as observed from Fig. 5(a), the membrane properties were also dominated by drying temperature. At a constant polymer content (5 wt.%), the lateral wicking time of membrane increased from 500 s to 707 s with the increase in drying temperature from 27°C to 53°C. The increase of temperature during dry phase inversion leads to the formation of membranes with smaller pores, lower membrane porosity and partial shrinkage of cell structures on the polymer matrix. This pore structure shrinkage and lower membrane porosity contribute to overall resistance of the membrane that hinders the liquid flow rate. Hence, higher lateral wicking time is needed. By changing the wicking medium, results show the obvious increasing trend of lateral wicking time with the increasing of drying temperature, as shown in Fig. 5(b). This further confirms that membrane morphology is the sole factor that promotes membrane performance in lateral liquid flow.

By changing both polymer concentration and drying temperature, very different membrane protein binding performances were observed (Fig. 6). Fig. 6 shows that at constant temperature, the membrane protein binding decreases with increasing polymer concentration. For example, at 40°C, protein binding of the membrane dropped from 3813 $\mu\text{g}/\text{cm}^3$ to 2965 $\mu\text{g}/\text{cm}^3$ when polymer concentration was increased from 4 wt.% to 6 wt.%. This suggests that at higher polymer concentration, the fast phase separation on the membrane outer layer and slow evaporation rate in the membrane inner layers forms a membrane surface with lower porosity and shrinking pore structure. This leads to a low surface protein binding value in accordance with Jansen et al. [17] who found the influence of polymer concentration on pore size and morphology of poly(ether ether ketone) membrane.

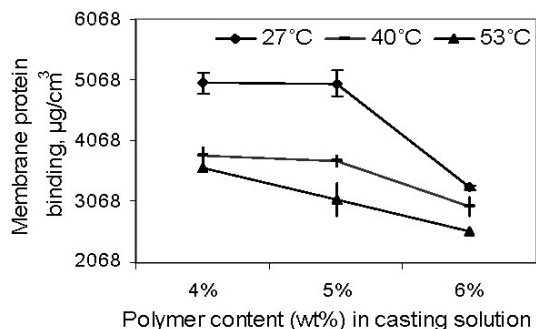


Fig. 6. Effects of casting polymer composition and casting condition (evaporation temperature) on membrane protein binding ability. Bars represent the standard error.

On the other hand, Fig. 6 shows that by increasing the drying temperature, the membrane protein binding ability was decreased. High drying temperatures are expected to improve the phase separation rate in the casting solution. A higher phase separation rate further increases the polymer concentration near to the membrane surface region and creates a resistance to solvent evaporation between the membrane inter layers [20]. This causes the formation of close pore structures on the membrane surface that reduces the membrane protein binding ability.

4. Conclusions

The effects of polymer composition and drying temperature on membrane morphology were investigated. Experimental results clearly demonstrate that final membrane structure and performances were significantly affected by the two aforesaid preparation conditions. Membranes with a mean pore diameter between 3.6 to 9.1 μm can be easily altered during the casting stage by varying the polymer concentration or by changing the drying temperature. Overall, this study provides a clear view on final membrane performances (lateral wicking speed and membrane protein binding ability) by identifying the interactions among the casting composition and casting process variable. The presence of low polymer concentration in casting solution results in favourable formation of larger membrane pores, higher membrane protein binding ability and shorter time for lateral liquid migration flow across membrane strips. In addition, membranes prepared from low drying temperature conditions create an open pore structure on the surface and increase the connection voids between membrane layers. Consequently, this results in lower resistance for the wicking medium to migrate in the membrane strip and increases membrane binding ability.

The above findings provide important insights into the relationship between membrane casting conditions and performance. This investigation should prove useful for the production of versatile NC membranes with longer operational life for lateral flow membrane applications.

Acknowledgement

The authors wish to thank the MOSTI Science Fund (03-01-05-SF0133) and MTDC research funding (BF/055-D) for its continuous financial support throughout this research.

References

- [1] W.O.K. Grabow, M.B. Taylor and J.C. De Villiers, New methods for the detection of viruses: Call for review of drinking water quality guidelines, *Water Sci. Technol.*, 43 (2001) 1.
- [2] W. Köhler, The search for typhoid bacilli in drinking and river waters, *Int. J. Med. Microbiol.*, 293 (2003) 385.
- [3] F.M. Schets, M. During, R. Italiaander, L. Heijnen, S.A. Rutjes, W.K. van der Zwaluw and A.M. de Roda Husman, *Escherichia coli* O157:H7 in drinking water from private water supplies in the Netherlands, *Water Res.*, 39 (2005) 4485.
- [4] M.A. Ali, A.Z. Al-Herrawy and S.E. El-Hawaary, Detection of enteric viruses, *Giardia* and *Cryptosporidium* in two different types of drinking water treatment facilities, *Water Res.*, 38 (2004) 3931.
- [5] W.-J. Gui, S.-T. Wang, Y.-R. Guo and G.-N. Zhu, Development of a one-step strip for the detection of triazophos residues in environmental samples, *Anal. Biochem.*, 377 (2008) 202.
- [6] P. Sithigorngul, S. Rukpratanporn, N. Pecharaburanin, P. Sukawat, S. Longyant, P. Chaivisuthangkura and W. Sithigorngul, A simple and rapid immunochromatographic test strip for detection of pathogenic isolates of *Vibrio harveyi*, *J. Med. Microbiol.*, 71 (2007) 256.
- [7] T.-H. Young and L.-W. Chen, Pore formation mechanism of membranes from phase inversion process, *Desalination*, 103 (1995) 233.
- [8] I. Pinnau and W.J. Koros, A qualitative skin layer formation mechanism for membranes made by dry/wet phase inversion, *J. Polym. Sci. Pt. B-Polym. Phys.*, 31 (1993) 419.
- [9] R.E. Kesting, *Synthetic Polymer Membranes: A Structural Perspective*, 2nd ed., Wiley, New York, 1985, p. 44.
- [10] D.M. Vaessen, A.V. McCormick and L.F. Francis, Effects of phase separation on stress development in polymeric coatings, *Polymer*, 43 (2002) 2267.
- [11] A.L. Ahmad, S.C. Low, S.R.A. Shukor and I. Asma, Synthesis and characterization of polymeric nitrocellulose membranes: Influence of additives and pore formers on the membrane morphology, *J. Appl. Polym. Sci.*, 108 (2008) 2550.
- [12] A.L. Ahmad, S.C. Low and S.R.A. Shukor, Effects of membrane cast thickness on controlling the macrovoid structure in lateral flow nitrocellulose membrane and determination of its characteristics, *Scr. Mater.*, 57 (2007) 743.
- [13] A.L. Ahmad, M. Sarif and S. Ismail, Development of an integrally skinned ultrafiltration membrane for wastewater treatment: effect of different formulations of PSf/NMP/PVP on flux and rejection, *Desalination*, 179 (2005) 257.
- [14] M.I. Mustaffar, A.F. Ismail and R.M. Illias, Study on the effect of polymer concentration on hollow fiber ultrafiltration membrane performance and morphology, *Regional Symp. Membr. Sci. and Technol.*, 2004.
- [15] M.M. Meier, L.A. Kanis and V. Soldi, Characterization and drug-permeation profiles of microporous and dense cellulose acetate membranes: influence of plasticizer and pore forming agent, *Int. J. Pharm.*, 278 (2004) 99.

- [16] S. Yamane, K. Takayama and T. Nagai, Effect of fractal dimension on drug permeation through porous ethylcellulose films, *J. Control Release*, 50 (1998) 103.
- [17] J.C. Jansen, M.G. Buonomenna, A. Figoli and E. Drioli, Asymmetric membranes of modified poly(ether ether ketone) with an ultra-thin skin for gas and vapour separations, *J. Membr. Sci.*, 272 (2006) 188.
- [18] N.A. Mohamed and A.O.H. Al-Dossary, Structure-property relationships for novel wholly aromatic polyamide-hydrazides containing various proportions of para-phenylene and meta-phenylene units III. Preparation and properties of semi-permeable membranes for water desalination by reverse osmosis separation performance, *Eur. Poly. J.*, 39 (2003) 1653.
- [19] S.A. Altinkaya, H. Yenal and B. Ozbas, Membrane formation by dry-cast process: Model validation through morphological studies, *J. Membr. Sci.*, 249 (2005) 163.
- [20] M.G. Buonomenna, P. Macchi, M. Davoli and E. Drioli, Poly(vinylidene fluoride) membranes by phase inversion: the role the casting and coagulation conditions play in their morphology, crystalline structure and properties, *Eur. Poly. J.*, 43 (2007) 1557.